

Experimental study of the flux Law of flat ceramic membranes under different pressures

Sun Chuanwen^a, Wang Haiqiao^a, Yu Qi^{b,*}, Chen Shiqiang^a, Li Xun^c and Wu Hanyang^d

^aSchool of Resources, Environment and Safety Engineering, Hunan University of Science and Technology, Xiangtan 411201, China

^bInstitute of Intelligent Manufacturing, Hunan Vocational Institute of Technology, Xiangtan 411201, China

^cSchool of Civil Engineering, Hunan University of Science and Technology, Xiangtan 411201, China

^dJiangxi Bocent Advanced Ceramics Co., Ltd., Pingxiang 337000, China

*Corresponding author. E-mail: 160101050002@mail.hnust.edu.cn

Abstract

The flux performance of ceramic membranes is the basis for their efficient use. To study ceramic membrane flux variation, different filtration operating conditions were tested and the functional relationship between the membrane's clean water flux and the operating pressure within a given range obtained. The membrane's critical pressure and flux were determined by using pressure increments, and the flux variation law under different pressures determined experimentally. Analysis of the flux law and the membrane parameters enabled establishment of the flux model of filtration process and a model of flux stabilization after the deposition layer formed. The applicability of the model was proved by comparing and verifying the experimental data.

Key words: critical pressure, flat ceramic membrane, flux changes, flux model, model validation

INTRODUCTION

Because of their excellent performance, ceramic membranes have been used widely for filtration and separation in recent years. Compared with organic membranes, ceramic membranes not only have stable chemical properties, but can also be cleaned and reused after contamination, and have high separation efficiency with good service life (Wang *et al.* 2015). The quality of municipal wastewaters, hospital wastewaters containing bacteria and chemical wastewaters are good after treatment by ceramic membrane, and meets the sewage discharge requirements (Xu *et al.* 2002, 2003; Wang *et al.* 2010; Chang *et al.* 2016). When a ceramic membrane is assembled into a membrane contactor or condenser, it performs well in resource recovery and removing harmful substances from flue gas (Cao *et al.* 2019; Huang *et al.* 2019). It has also been found that ceramic membranes can be used to recover heat-emitting pollutants at high recovery rates and are effective in reducing the waste of resources (Chen *et al.* 2017a; Dilaver *et al.* 2018).

Ceramic membranes are used widely in various fields, but most current studies relate to phase separation and material collection (Chen *et al.* 2017b; Li *et al.* 2017; Zheng *et al.* 2018), as well as the effects of operating parameters on membrane flux and material removal rates (Lu *et al.* 2009; Zhang *et al.* 2016; Zhou *et al.* 2017). These studies can provide experimental parameters for operations using the same or similar filtration conditions, while there is no systematic theory for ceramic membrane contamination and flux variation under different conditions – that is, there is no quantitative method for determining membrane contamination and/or flux changes. In this

study, ceramic membrane flux variations under different operating pressures and the critical operating pressures were determined experimentally, enabling determination of the optimum filtration pressure and maximizing filtration efficiency. At the same time, by analyzing fouling on the membrane surface and the flux curve, a flux change model was established. This enabled the membrane's flux change rule to be described quantitatively, reflecting the membrane's fouling, and providing a theoretical basis for determining cleaning time, as well as for wide application of ceramic membranes.

MEMBRANE FLUX THEORY

Filtration flux model

According to the principle of filtration, ceramic membranes will not be polluted when filtering clean water, and the flux depends on the membrane parameters and operating pressures. By analyzing the micro-parameters of a sintered ceramic membrane, it can be shown that the membrane's resistance is determined by the filtration specific resistance and the thickness of the separation layer, and that the filtration resistance is related to the average membrane pore diameter and the porosity of the membrane formed. Thus, the ceramic membrane's resistance is a function of the average membrane pore size, its porosity and the thickness of separation layer (Xu 2017). The relationship is shown in Equation (1):

$$R_{m0} = \frac{k_1 \cdot (1 - \varepsilon_{m0})^2}{d_m^{k_2} \cdot \varepsilon_{m0}^3} \cdot L \quad (1)$$

where R_{m0} is the self-resistance of the membrane (m^{-1}); k_1 and k_2 are undetermined model parameters obtained by curve-fitting; d_m is the pore size of the membrane (m); ε_{m0} is the porosity of the newly formed membrane; and L is the thickness of the membrane separation layer (m).

When the resistance is determined, the flux can be calculated directly using Darcy's formula. However, when a ceramic membrane is used in practical filtration and separation, the pollutants in the filtrate will enter the membrane pores and/or deposit on the membrane surface, causing fouling, resulting in the flux decreasing during filtration and affecting the normal filtration process (Lv 2016). Filtration contamination is currently judged by measuring the pressure differential across the membrane. However, the fouling layer on the membrane surface changes during filtration and its parameters cannot be determined during the process. Therefore, the law of filtration flux change with time can only be judged by experience, and cannot be calculated quantitatively.

The ceramic membrane's separation layer is formed by the accumulation of minute particles during sintering, like the fouling layer formed on the contaminated ceramic membrane's surface. Therefore, taking into account the relationship between the membrane's self-resistance and its structural parameters, the particles deposited on the membrane surface and those forming its separation layer can be considered integral, when calculating the flux with fouling at different times, and membrane resistance is still expressed as a function of the membrane's own structural parameters.

The ceramic membrane filtration flux variation law says that the trend of the change of flux with time is approximately exponential. Based on the view that the particles deposited on the membrane surface and those in the membrane separation layer can be regarded as a whole, a flux model based on the membrane resistance and flux variation during filtration and separation is proposed according to Darcy's formula – Equation (2), which can be used to determine the flux of different filtration and separation processes at different times.

$$J(t) = a \cdot \frac{\Delta P}{\mu \cdot R_{m0}} \cdot e^{-b \cdot t} + c \quad (2)$$

where $J(t)$ is the membrane flux at different times ($\text{L}\cdot\text{h}^{-1}\cdot\text{m}^{-2}$); μ the hydrodynamic viscosity ($\text{Pa}\cdot\text{s}$); ΔP the filtration pressure (kPa); and a , b and c the experimental parameters, obtained by curve-fitting the experimental data.

Flux model after deposit formation and flux stabilization

In the later stages of filtration, the amount of particulate material deposited on the membrane surface and the solute returned to the filtrate due to concentration polarization reach dynamic equilibrium, and the particles deposited on the membrane surface form a stable layer (Field *et al.* 1995). Analysis of substance concentrations in the surface deposition layer shows that particulate concentration in the fouling layer is at its highest at the membrane surface, and gradually falls away as the thickness of the fouling layer increases, until it is similar to that in the fluid being filtered – see Figure 1.

According to the material balance equation – Equation (3) – the solid-phase particles are balanced when the filtrate passes through the membrane surface:

$$J \cdot c_p = J \cdot c(x) - D \cdot \frac{dc(x)}{dx} \quad (3)$$

Figure 1 shows that the boundary conditions are: $\begin{cases} x = 0, c(x) = c_m \\ x = h, c(x) = c_b \end{cases}$, by integrating Equation (3) and substituting the boundary conditions, Equation (4) can be obtained:

$$\frac{c_b - c_p}{c_m - c_p} = e^{\frac{J \cdot h}{D}} \quad (4)$$

Defining the mass transfer coefficient $k = \frac{D}{h}$, and the intrinsic retention rate $R = 1 - \frac{c_p}{c_m}$, and substituting them into Equation (4), yields Equation (5):

$$\frac{c_b}{c_m} = R \cdot e^{\frac{J}{k}} - R + 1 \quad (5)$$

Compared with the solute concentrations in the filtrate and the membrane deposition layer, that the filtrate after filtration is negligible; that is, $c_b = 0$, $R = 1$. Where D is the solute diffusion coefficient ($\text{cm}^2\cdot\text{s}^{-1}$), which can be estimated approximately using Equation (6) when the flux is low (Wilke & Chang 1955):

$$D = 7.4 \times 10^{-8} \times \frac{(\varphi \cdot M)^{0.5} \cdot T}{\mu \cdot V^{0.6}} \quad (6)$$

Therefore, the ceramic membrane flux model expression after fouling and flux stabilization can be obtained as Equation (7) after sorting out Equation (5):

$$J = \frac{D}{h} \cdot \ln \frac{c_m}{c_b} \quad (7)$$

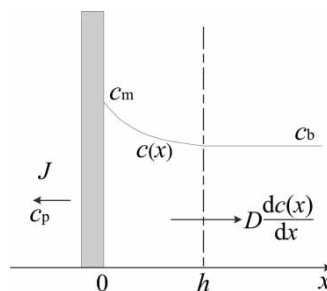


Figure 1 | Concentration polarization analysis of the membrane surface.

where φ is the association coefficient (which is 2.6 here); μ the solution's dynamic viscosity (cp); M the molar mass of water; T the absolute temperature (K); V the molecular volume of filtrate particles – estimated as 6.17 by the Tyn-Calus method (Yaws & Narasimhan 2009); c_b the solute concentration in the filtrate ($\text{kg}\cdot\text{m}^{-3}$); c_m the solute concentration in the membrane surface of the deposition layer ($\text{kg}\cdot\text{m}^{-3}$) – according to Davis (1992), for spherical particles with different size distributions, c_m is about 0.8 to 0.9 ($\text{kg}\cdot\text{m}^{-3}$); and h is the deposition layer thickness (m).

MATERIALS AND METHODS

Materials

The flat ceramic membrane used in the experiment came from Bocent Advanced Ceramics Co., Ltd in Pingxiang City, Jiangxi Province, China. The principal components are sintered Al_3O_2 and SiO_2 , and the average pore diameter is 0.1 μm with porosity about 0.35 to 0.38. The filtrate used was wastewater contaminated mainly with coal dust and the clean water was Watson's distilled water (Watson, Hong Kong, China). The filtration mode adopted was external inlet and internal suction, and the operating pressure was generated by the head differential, to ensure operating stability.

The negative pressure suction filter used comprised mainly a filter tank and clean water tank and the ceramic membrane components. The ceramic membrane module was vertical in filtration mode, and filtration was static (Figure 2). One end of the filter tube was connected to the ceramic membrane outlet and the other to the clean water tank. The filter head differential was controlled by adjusting the filter tube length, and was determined with a tape measure. The flow rate at any time was measured as the volume captured in a cylinder from 5 seconds before to 5 seconds after that time, and then calculated in relation to the membrane's effective filtration area. The accuracies of the tape measure, measuring cylinder and timer used were 1 mm, 1 ml and 0.01 secs, respectively.

Experimental process

The experiment was designed to analyze the ceramic membrane's performance under differing operating conditions. The main contents and steps were:

Measurement of clean water flux

Membranes are not contaminated by clean water, so the flux was constant during filtration. By measuring the clean water flux under different operating pressures, the membrane's self-resistance and the relationship between clean water flux and operating pressures could be determined. Distilled water was used to measure the membrane's clean water flux. In this step, a known volume of distilled water was put into the filter tank and the liquid level remained constant. The filter tube length was adjusted so that one end was connected to the water purifier and the other was 1 m from the vertical height of the liquid level of the filter tank, generating 10 kPa head, driving the distilled water from the filter tank to the clean water tank through the ceramic membrane. When the flow rate had stabilized, it was measured for 10 seconds every 2 minutes. The measurements were repeated 5 times over 8 minutes and the average value taken as the membrane's clean water flux at this pressure. The length of the filter tube was then adjusted, and the membrane's clean water fluxes at operating pressures of 20, 30 and 40 kPa were measured in the same way (see Figure 3).

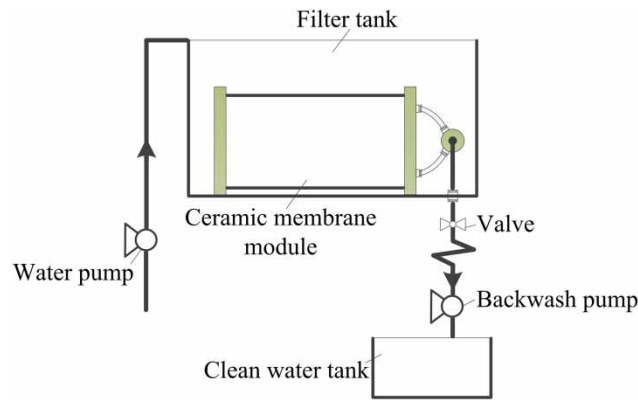


Figure 2 | Schematic diagram of the experimental device.

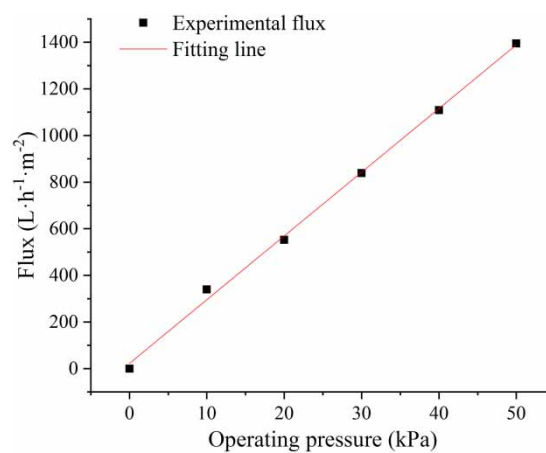


Figure 3 | Variation of clean water flux with pressure in a ceramic membrane with 0.1 μm pores.

Determination of critical pressure and flux

When *Field et al. (1995)* proposed the concept of critical flux, they believed that a critical flux existed in membrane systems during filtration. When the system was operated below this flux, the membrane would not become substantially contaminated for a considerable period of time, but membrane fouling would occur very quickly during operation above it. Determination of the critical flux could set a suitable operating range for the system, while ensuring efficient operation and production (*Xu 2008*).

The membrane's critical pressure and flux were measured using incremental pressure changes. The filter system's operating pressure was set at 2.5 kPa and, when the flow rate was stable, the 10-second volume was determined every 2 minutes over 8 minutes. If the flux remained constant during this time, the operating pressure was increased by 1.5 kPa. Pressure increases and measurements continued in this way until the flux fell significantly when the pressure was increased, and it was considered that flux, J_m , and pressure, P_m , were approximately at critical levels. It was important that the stages should not be too long, to avoid adsorptive contamination occurring, as that could affect the measurement of flux.

Flux variation at different operating pressures

Operating pressures of 2.5, 6, 8 and 11 kPa were used in the filtration experiments, and the flux variation with filtration time observed. The ceramic membrane was cleaned between experiments – that is, when each set of measurements was complete. The membrane was cleaned by backwashing with

filtrate from the clean water tank for 30 minutes, then soaking it in 1% NaOH and 0.3% HCl solutions for 1 hour each. Finally, the membrane was replaced in the filter tank of the system – Figure 2 – and backwashed for a further 30 minutes with filtrate from the clean water tank. For this filtrate, the membrane flux was restored to its original level by this method.

RESULTS AND ANALYSIS

The law of clean water flux

Analysis of the clean water flux data enabled a relationship to be derived between clean water flux and operating pressure – Figure 3:

As can be seen, the ceramic membrane's flux when filtering clean water is affected only by the membrane's self-resistance and the operating pressure. The clean water flux increases with increasing operating pressure when the self-resistance is constant. The membrane's clean water flux is approximately proportional to the operating pressure within a given range. By linear fitting of the data, the functional relationship of the membrane's clean water flux with operating pressure was shown to be $y = 27.33x + 22$. The formula can only be applied within a certain range of operating pressures, however, as when the pressure exceeds the membrane's strength, the membrane structure will be damaged and the formula will no longer meet the requirements.

Determination of the critical flux and pressure

Different ceramic membranes have different critical fluxes and pressures when filtering different influents. The determination of critical flux and pressure is significant for slowing down membrane fouling and improving filtration efficiency (Liu *et al.* 2017). The ceramic membrane's critical flux and pressure were measured as noted above, and the pressure gradient ΔP for each increment was 1.5 kPa. The experimental data were analyzed and plotted as the point-line graph in Figure 4.

Figure 4 shows that when the operating pressure is below 4 kPa, the membrane's flux is basically stable at each pressure stage for some period of time, and the flux increases correspondingly with increasing pressure, but also remains stable. Thus it is clear that the membrane has not been truly contaminated at this operating pressure during this time. When the operating pressure is increased to 5.5 kPa, the membrane flux increases initially from 141 to 180 $\text{L}\cdot\text{h}^{-1}\cdot\text{m}^{-2}$, but then decreases gradually as filtration

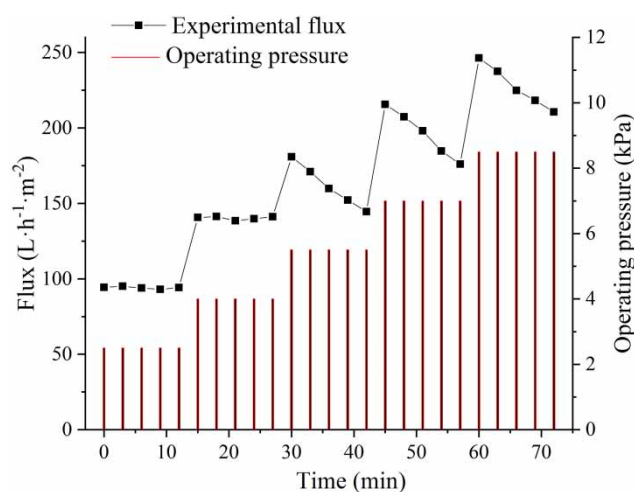


Figure 4 | Determination of critical pressure (flux) of ceramic membranes.

proceeds to about $145 \text{ L}\cdot\text{h}^{-1}\cdot\text{m}^{-2}$ after a few minutes, indicating that the membrane is becoming fouled at this operating pressure. As the operating pressure is increased, the flux shows the same trend with operating time, so there is a critical pressure between 4 and 5.5 kPa, below which the membrane will not be contaminated/fouled and the flux will remain stable. When the pressure is raised above the critical level, the flux increases correspondingly, but decreases gradually during filtration as membrane fouling occurs. In this study, the average operating pressure before and after the flux change was taken as the membrane's critical pressure and is 4.75 kPa, with a corresponding critical flux of $160.56 \text{ L}\cdot\text{h}^{-1}\cdot\text{m}^{-2}$.

Flux variation under different operating pressures

The experimental flux measurements below and above the critical pressure from the study are shown in Figure 5.

Figure 5 shows that when filtration is conducted below the critical pressure (i.e. the operating pressure is 2.5 kPa), the flux falls relatively slowly. After more than two hours the flux had fallen from the original $95 \text{ L}\cdot\text{h}^{-1}\cdot\text{m}^{-2}$ to about 54 (black line). In contrast, when the membrane is operated above the critical pressure, the flux falls rapidly over a short period of time and the higher the operating pressure the faster the rate of decrease. This is because the higher operating pressure and greater flux lead to faster deposition of contaminants on the membrane surface, so that the flux decreases faster (Li *et al.* 2013). This also confirms that membrane fouling is relatively slower below the critical pressure, and that increasing the operating pressure will make fouling occur more quickly. After a period of operation, the thickness of fouling contaminants on the membrane surface will stabilize; that is, their hydraulic resistance will remain unchanged at a certain value, and the flux will decrease no further. In Figure 6, the membrane surface (a) and (b), and cross-sections (c) and (d) are shown at 2 k magnification before and after filtration at 6 kPa. The images were taken with an FEI-Q45 scanning electron microscope (FEI Company, Hillsboro City, America).

In Figure 6 it can be seen that the contaminated membrane surface is smoother before filtration (image a) than after (b), when it is covered with irregular particles – the contaminants intercepted by the membrane. Image (c) shows the surface before filtration, whereas (d) shows a large amount of particles deposited on the membrane surface to the right of the dotted line and that the membrane's structural state has changed.

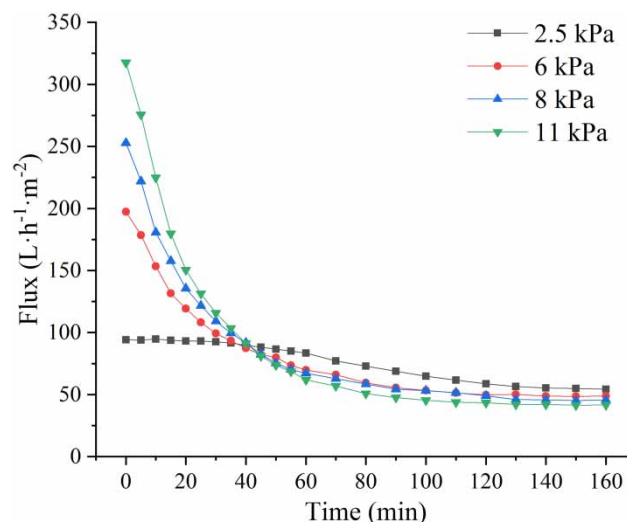


Figure 5 | Ceramic membrane flux curves time under different operating pressure.

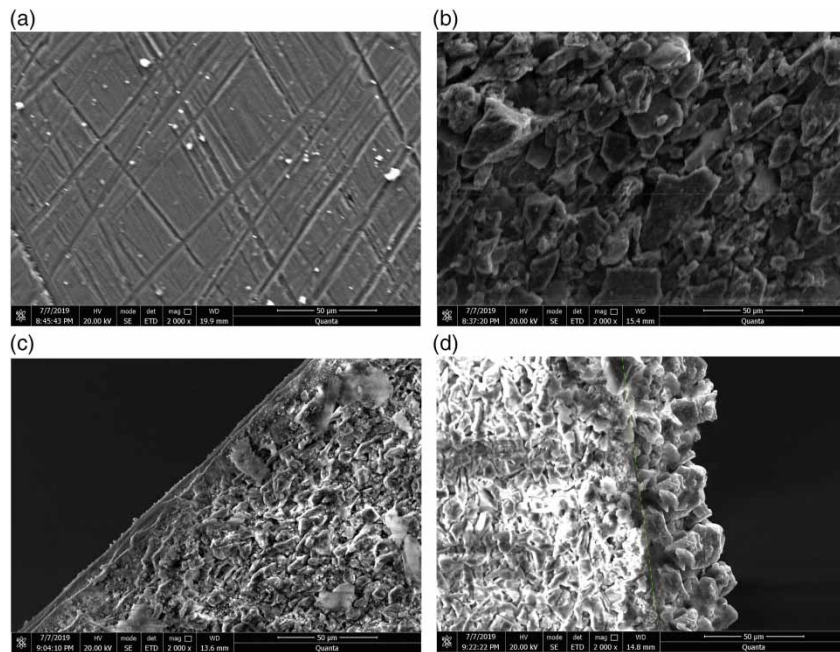


Figure 6 | Comparison of membrane surface and cross-section before ((a) and (c)) and after ((b) and (d)) operation.

FLUX MODEL VERIFICATION

Validation of flux model in filtration

The membrane filtration flux model was established as in Equation (2), which was based on the membrane's structural parameters and the flux variation law in filtration. The model could be used to determine the flux/time relationship without analyzing the properties of the influent or membrane fouling.

The flux model was verified using the ceramic membrane's time-varying flux data at 6 kPa operating pressure. The fitting parameters were $a = 0.93$, $b = 0.0421$, $c = 50.34$, and the correlation coefficient $R^2 = 0.99711$. Figure 7 is a comparison between the fitting curve and the experimental data.

The versatility of Equation (2) was verified using the membrane fluxes found under different operating pressures. The fitting curve/experimental flux relationships at 8 (a) and 11 kPa (b) are shown in Figure 8.

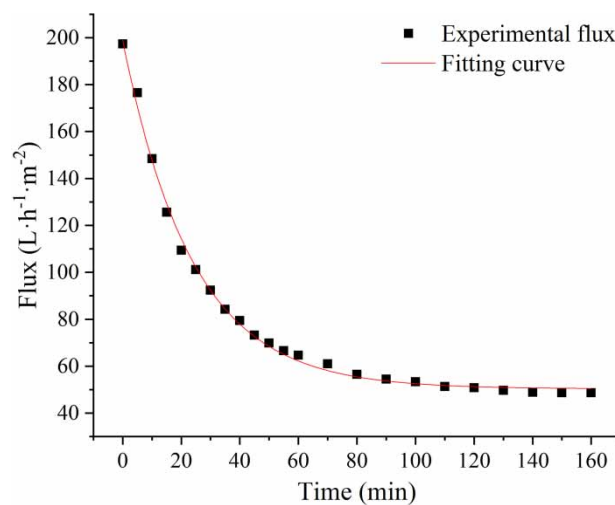


Figure 7 | Comparison between fitting curve and experimental data.

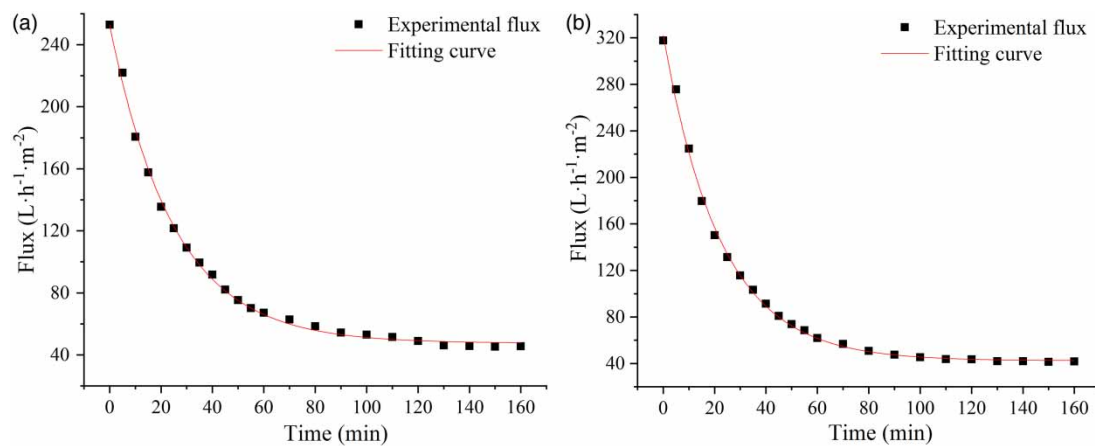


Figure 8 | Experimental fluxes and fitting curves at (a) 8 and (b) 11 kPa.

Table 1 | Errors between the modeled and experimental flux values

Operating pressure (kPa)	6	8	11
Errors (%)	7.48	5.01	7.08

The fitting curves keep the same trend as the experimental fluxes and fit well, so the established flux model enables the calculation of membrane fluxes at different times and operating pressures, and can be used to determine flux changes at different times.

Flux model verification after membrane fouling and flux stabilization

In late-stage filtration, membrane fouling was stable and the fouling-layer resistance was constant, so the membrane's flux stayed the same. The stable flux values obtained from the model after fouling were compared with those measured under different operating conditions. When the stable, measured flux values measured under different operating conditions were compared with those calculated by the flux model, some small but acceptable differences were found – see Table 1. In other words, the flux model is verified.

CONCLUDING REMARKS

- (1) Based on analysis of the membrane's structural parameters and the particles on the fouled membrane surface, and the filtration process flux variation law, models were established for both filtration flux change and flux stabilization after fouling.
- (2) Changes of the membrane's clean water flux with operating pressure were measured, and the functional relationship of the clean water flux with operating pressure determined by fitting and analyzing the experimental data.
- (3) The membrane's critical flux and operating pressure were measured, as well as the relationship between its flux and time under different operating pressures, showing that the flux decreased slowly with filtration time below the critical pressure. The model was also validated using experimental data above the critical pressure and its applicability proved.

REFERENCES

- Cao, Y., Wang, L., Ji, C., Huang, Y. Z., Xue, Z. L., Lu, J. M. & Qi, H. 2019 Pilot-scale application on dissipation of smoke plume from flue gas using ceramic membrane condensers. *CIESC Journal* **70**(6), 2192–2201.
- Chang, H. C., Cao, J. S. & Zhou, B. Y. 2016 Application of ceramic membrane bioreactor in wastewater treatment of infectious disease hospital. *Water Purification Technology* **35**(5), 100–103 + 113.
- Chen, H. P., Zhou, Y. N., Cao, S. T., Li, X., Su, X., An, L. S. & Gao, D. 2017a Heat exchange and water recovery experiments of flue gas with using nanoporous ceramic membranes. *Applied Thermal Engineering* **110**, 686–694.
- Chen, P. L., Ma, X., Zhong, Z. X., Zhang, F., Xing, W. H. & Fan, Y. Q. 2017b Performance of ceramic nanofiltration membrane for desalination of dye solutions containing NaCl and Na₂SO₄. *Desalination* **404**, 102–111.
- Davis, R. H. 1992 Modeling of fouling of crossflow microfiltration membranes. *Separation and Purification Methods* **21**(2), 75–126.
- Dilaver, M., Hocaoglu, S. M., Soydemir, G., Dursun, M., Keskinler, B., Koyuncu, I. & Agtas, M. 2018 Hot wastewater recovery by using ceramic membrane ultrafiltration and its reusability in textile industry. *Journal of Cleaner Production* **171**(C), 220–233.
- Field, R. W., Wu, D., Howell, J. A. & Gupta, B. B. 1995 Critical flux concept for microfiltration fouling. *Journal of Membrane Science* **100**(3), 259–272.
- Huang, Y., Xu, P., Kong, X. L., Zhou, X., Gao, X. Y., Fu, K. Y., Qiu, M. H. & Luo, P. 2019 Mass transfer enhancement of SO₂ absorption via ceramic membrane contactor in wetting mode. *Acta Scientiae Circumstantiae* **39**(6), 1952–1958.
- Li, C. Y., Li, X. Q., Jiang, M. Z., Hong, Y. B. & Fang, Y. Z. 2013 Analysis of membrane fouling and mechanism of protein and Maillard products in fermentation broth. *Membrane Science and Technology* **33**(5), 14–18.
- Li, B., Li, Y. Q., Pu, J. W., Huang, S. S., Guo, L. W., Zhu, H. X. & Duan, J. A. 2017 Study on the treatment of Mailuoning's wastewater by ceramic membrane based on resource utilization. *Membrane Science and Technology* **37**(6), 107–113.
- Liu, C., Lv, X. L., Wu, C. R., Wang, X., Gao, Q. J., Chen, H. Y. & Jia, Y. 2017 Discussion on critical operating flux of ultrafiltration membrane. *Membrane Science and Technology* **1**, 23–26.
- Lu, H. J., Wang, J., Luo, W. H. & Chen, J. H. 2009 Study on performance parameters of ceramic membranes. *Environmental Engineering* **27**(S1), 163–165.
- Lv, D. W. 2016 *Study on Membrane Fouling Mechanism and Anti-Fouling Modification in Ceramic Ultrafiltration Membrane Separation of Emulsion oil*. PhD thesis, Harbin Institute of Technology, Harbin, China.
- Wang, S. X., Li, Y., Li, J. X. & Zhou, X. 2010 Application of ceramic membranes to the advanced treatment of chemical wastewater. *Industrial Water Treatment* **30**(3), 79–81.
- Wang, Y. Q., Hou, J. P., Chang, Q. B., Yang, K. & Zhou, J. E. 2015 Effect of particle size gradients of alumina powders on the pore size distribution of ceramic membrane. *Journal of Synthetic Crystals* **44**(11), 3245–3249.
- Wilke, C. R. & Chang, P. 1955 Correlation of diffusion coefficients in dilute solutions. *Aiche Journal* **1**(2), 264–270.
- Xu, W. Y. 2008 *Experimental Study on Treatment of Municipal Domestic Wastewater by A/O-Dynamic Membrane Bioreactor*. MA thesis, Southeast University, Nanjing, China.
- Xu, N. P. 2017 *Design, Preparation and Application of Ceramic Membrane Material Oriented to Application Process*, 1st edn. Science Press, Beijing, China.
- Xu, N., Xing, W. H., Xu, N. P. & Shi, J. 2002 Application of turbulence promoters in ceramic membrane bioreactor used for municipal wastewater reclamation. *Journal of Membrane Science* **210**(2), 307–313.
- Xu, N., Xing, W. H., Xu, N. P. & Shi, J. 2003 Study on ceramic membrane bioreactor with turbulence promoter. *Separation and Purification Technology* **32**(1), 403–410.
- Yaws, C. L. & Narasimhan, P. K. 2009 Chapter 2-Critical properties and acentric factor – inorganic compounds. In: *Thermophysical Properties of Chemicals and Hydrocarbons*, pp. 96–105.
- Zhang, J. B., Zeng, J. X., Zhang, X. J., Shen, S. H., Yu, X., Qian, Z. H., Zhang, P. & Tian, J. 2016 Treatment of electroplating wastewater containing nickel ions with ceramic membranes. *Journal of Environmental Engineering* **10**(4), 1699–1705.
- Zheng, J. J., Wang, Z. W., Ma, J. X., Xu, S. P. & Wu, Z. C. 2018 Development of an electrochemical ceramic membrane filtration system for efficient contaminant removal from waters. *Microfiltration* **52**(7), 4117–4126.
- Zhou, Z., Yao, J. L., Pang, Z. B., Liu, B. & Zhang, X. 2017 Effect of transmembrane pressure and crossflow velocity on membrane fouling using magnetic flocculation pretreatment. *Environmental Engineering* **35**(6), 10–14.